bioRxiv preprint doi: https://doi.org/10.1101/2020.04.16.045419; this version posted April 18, 2020. The copyright holder for this preprint (which was not certified by peer review) is the author/funder, who has granted bioRxiv a license to display the preprint in perpetuity. It is made available under aCC-BY 4.0 International license.

Synthetic nanobodies targeting the SARS-CoV-2 receptor-binding domain

Justin D. Walter[1,#], Cedric A.J. Hutter[1,#], Iwan Zimmermann[1,2], Jennifer Earp[1], Pascal Egloff[1,2], Michèle Sorgenfrei[1], Lea M. Hürlimann[1], Imre Gonda[1], Gianmarco Meier[1], Sille Remm[1], Sujani Thavarasah[1], Philippe Plattet[3], Markus A. Seeger[1,*]

[1]Institute of Medical Microbiology, University of Zurich, Switzerland

[2]Linkster Therapeutics AG, Zurich, Switzerland

[3]Division of Experimental and Clinical Research, Vetsuisse Faculty, University of Bern, Switzerland

[#]Equal contribution

[*]Corresponding author: m.seeger@imm.uzh.ch

ABSTRACT

The COVID-19 pandemic, caused by the novel coronavirus SARS-CoV-2, has resulted in a global health and economic crisis of unprecedented scale. The high transmissibility of SARS-CoV-2, combined with a lack of population immunity and prevalence of severe clinical outcomes, urges the rapid development of effective therapeutic countermeasures. Here, we report the generation of synthetic nanobodies, known as sybodies, against the receptor-binding domain (RBD) of SARS-CoV-2. In an expeditious process taking only twelve working days, sybodies were selected entirely *in vitro* from three large combinatorial libraries, using ribosome and phage display. We obtained six strongly enriched sybody pools against the isolated RBD and identified 63 unique anti-RBD sybodies which also interact in the context of the full-length SARS-CoV-2 spike protein. It is anticipated that compact binders such as these sybodies could feasibly be developed into an inhalable drug that can be used as a convenient prophylaxis against COVID-19. Moreover, generation of polyvalent antivirals, via fusion of anti-RBD sybodies to additional small binders recognizing secondary epitopes, could enhance the therapeutic potential and guard against escape mutants. We present full sequence information and detailed protocols for the identified sybodies, as a freely accessible resource. This report will be updated as we further characterize the identified sybodies, in terms of affinities, scaled-up purification yields, and their potential to neutralize SARS-CoV-2 infections.

bioRxiv preprint doi: https://doi.org/10.1101/2020.04.16.045419; this version posted April 18, 2020. The copyright holder for this preprint (which was not certified by peer review) is the author/funder, who has granted bioRxiv a license to display the preprint in perpetuity. It is made available under aCC-BY 4.0 International license.

INTRODUCTION

The ongoing pandemic arising from the emergence of the 2019 novel coronavirus, SARS-CoV-2, demands urgent development of effective antiviral therapeutics. Several factors contribute to the adverse nature of SARS-CoV-2 from a global health perspective, including the absence of herd immunity [1], high transmissibility [2, 3], the prospect of asymptomatic carriers [4], and a high rate of clinically severe outcomes [5]. Moreover, a vaccine against SARS-CoV-2 is unlikely to be available for at least 12-18 months [6], despite earnest development efforts [7, 8], making alternative intervention strategies paramount. In addition to offering relief for patients suffering from the resulting COVID-19 disease, therapeutics may also reduce the viral transmission rate by being administered to asymptomatic individuals subsequent to probable exposure [9]. Finally, given that SARS-CoV-2 represents the third global coronavirus outbreak in the past 20 years [10, 11], development of rapid therapeutic strategies during the current crises could offer greater preparedness for future pandemics.

Akin to all coronaviruses, the viral envelope of SARS-CoV-2 harbors protruding, club-like, multidomain spike proteins that provide the machinery enabling entry into human cells [12-14]. The spike ectodomain is segregated into two regions, termed S1 and S2. The outer S1 subunit of SARS-CoV-2 is responsible for host recognition via interaction between its C-terminal receptor-binding domain (RBD) and human angiotensin converting enzyme 2 (ACE2), present on the exterior surface of airway cells [14, 15]. While there is no known host-recognition role for the S1 N-terminal domain (NTD) of SARS-CoV-2, it is notable that S1 NTDs of other coronaviruses have been shown to bind host surface glycans [12, 16]. In contrast to spike region S1, the S2 subunit contains the membrane fusion apparatus, and also mediates trimerization of the ectodomain [12-14]. Prior to host recognition, spike proteins exist in a metastable pre-fusion state wherein the S1 subunits lay atop the S2 region and the RBD oscillates between “up” and “down” conformations that are, respectively, accessible and inaccessible to receptor binding [12, 17, 18]. After receptor engagement and cleavage between S1 and S2 subunits by host proteases, the S2 subunit undergoes dramatic conformational changes from the pre-fusion to the post-fusion state. Such structural rearrangements are associated with the merging of the viral envelope with host membranes, thereby allowing injection of the genetic information into host cells [19, 20].

Coronavirus spike proteins are highly immunogenic [21], and several experimental approaches have sought to target this molecular feature for the purpose of viral neutralization [22]. The high specificity, potency, and modular nature of antibody-based antiviral therapeutics has shown exceptional promise [23-25], and the isolated, purified RBD has been a popular target for the development of anti-spike antibodies against pathogenic coronaviruses [26-29]. However, binders against the isolated RBD may not effectively engage the aforementioned pre-fusion conformation of the full spike, which could account for the poor neutralization ability of recently described single-domain antibodies that were raised against the RBD of SARS-CoV-2 [30]. Therefore, to better identify molecules with qualities befitting a drug-like candidate, it would be advantageous to validate RBD-specific binders in the context of the full, stabilized, pre-fusion spike assembly [13, 31].

Single domain antibodies based on the variable VHH domain of heavy-chain-only antibodies of camelids – generally known as nanobodies – have emerged as a broadly utilized and highly successful antibody fragment format [32]. Nanobodies are small (12-15 kDa), stable, and inexpensive to produce in bacteria and yeast [33], yet they bind targets in a similar affinity range as conventional antibodies. Due to their minimal size, they are particularly suited to reach hidden epitopes such as crevices of

bioRxiv preprint doi: https://doi.org/10.1101/2020.04.16.045419; this version posted April 18, 2020. The copyright holder for this preprint (which was not certified by peer review) is the author/funder, who has granted bioRxiv a license to display the preprint in perpetuity. It is made available under aCC-BY 4.0 International license.

target proteins [34]. We recently designed three libraries of synthetic nanobodies, termed sybodies, based on elucidated structures of nanobody-target complexes (Fig. 1A) [35, 36]. Sybodies can be selected against any target protein within twelve working days, which is considerably faster than natural nanobodies, which requires the repetitive immunization during a period of two months prior to binder selection by phage display [36] (Fig. 1C). A considerable advantage of our platform is that sybody selections are carried out under defined conditions — in case of coronavirus spike proteins, this offers the opportunity to generate binders recognizing the metastable pre-fusion conformation [13, 14]. Finally, due to the feasibility of inhaled therapeutic nanobody formulations [37], virus-neutralizing sybodies could offer a convenient and direct means of prophylaxis.

Here, we provide a preliminary report of the *in vitro* selection and identification of sybodies against the RBD of SARS-CoV-2. Two independently prepared RBD constructs were used for *in vitro* sybody selections, and resulting single clones that could bind the full spike protein were sequenced. We present all sequences for these clones, along with detailed protocols to enable the community to freely produce and further characterize these SARS-CoV-2 binders. This manuscript will be updated and amended as we continue analysis of these constructs, which will include ACE2 competition assays, pseudovirus neutralization experiments, and binding kinetics for the isolated RBD as well as the pre-fusion-stabilized spike assembly.

RESULTS AND DISCUSSION

Purification and biotinylation of target proteins

Based on sequence alignments with isolated RBD variants from SARS-CoV-1 that were amenable to purification and crystallization [29, 38], a SARS-CoV-2 RBD construct was designed, consisting of residues Pro330—Gly526 fused to venus YFP (RBD-vYFP). This construct was expressed and secreted from Expi293 cells, and RBD-vYFP was extracted directly from culture medium supernatant using an immobilized anti-GFP nanobody [39], affording a highly purified product with negligible background contamination. Initial efforts to cleave the C-terminal vYFP fusion partner with 3C protease resulted in unstable RBD, so experiments were continued with full RBD-vYFP fusion protein. To account for the presence of the vYFP fusion partner, a second RBD construct, consisting of a fusion to murine IgG1 Fc domain (RBD-Fc), was commercially acquired. To remove any trace amines, buffers were exchanged to PBS via extensive dialysis. Proteins were chemically biotinylated, and the degree of biotinylation was assessed by a streptavidin gel-shift assay and found to be greater than 90 % of the target proteins [40]. We note that while both RBD fusion proteins were well-behaved, a commercially acquired purified full-length SARS-CoV-2 spike protein was found to be aggregation-prone. Efforts are currently underway to produce a validated engineered spike protein containing mutations which are known to stabilize the pre-fusion state, as well as a C-terminal trimerization motif [13, 14, 31]. Therefore, all experiments presented herein pertaining to full-spike interactions will be replicated with the stabilized spike variant.

Sybody selections

Since both our RBD constructs bear additional large folded proteins (Fc of mouse IgG1 and vYFP, respectively), sybody selections were carried out with a “target swap” (Fig. 1B). Hence, selections with

bioRxiv preprint doi: https://doi.org/10.1101/2020.04.16.045419; this version posted April 18, 2020. The copyright holder for this preprint (which was not certified by peer review) is the author/funder, who has granted bioRxiv a license to display the preprint in perpetuity. It is made available under aCC-BY 4.0 International license.

the three sybody libraries (concave, loop and convex) were started with the RBD-vYFP construct using ribosome display, and the RBD-Fc construct was then used for the two phage display rounds (selection variant 1: RBD-vYFP/RBD-Fc/RBD-Fc) and *vice versa* (selection variant 2: RBD-Fc/RBD-vYFP/RBD-vYFP). Hence, there were a total of six selection reactions (Table 1, Fig. 1B). To increase the average affinity of the isolated sybodies, we included an off-rate selection step using the pre-enriched purified sybody pool after phage display round 1 as competitor. To this end, sybody pools of all three libraries of the same selection variant were sub-cloned from the phage display vectors into the sybody expression vector pSb_init. Subsequently, the two separate pools (all sybodies of selection variants 1 and 2, respectively) were expressed and purified. The purified pools were then added to the panning reactions of the respective selection variant in the second phage display round. Thereby, re-binding of sybody-phage complexes with fast off-rates was suppressed. Enrichment of sybodies against the RBD was monitored by qPCR. Already in the first phage display round, the concave and loop sybodies of selection variant 2 showed enrichment factors of 7 and 3, respectively (Table 1). After the second phage display round (which included the off-rate selections step), strong enrichment factors in the range of 10-263 were determined.

Sybody identification by ELISA

After sub-cloning the pools from the phage display vector pDX_init into the sybody expression vector pSb_init, 47 clones of each of the 6 selections reactions (Table 1, Fig. 1B) were picked at random and expressed in small scale. Our standard ELISA was performed using RBD-vYFP (RBD), spike ectodomain containing S1 and S2 (ECD) and maltose binding protein (MBP) as unrelated dummy protein. As outlined in the materials and methods, ELISA analysis revealed very high hit rates for the RBD and the ECD ranging from 81 % to 100 % and 66 % to 96 %, respectively (Fig. 2, Table 1). The majority of the sybodies giving an ELISA signal to the RBD also gave a clear signal the full-length spike protein (Fig. 2). However, there was a total of 44 hits that only gave an ELISA signal for RBD-vYFP, but not for the ECD. This could be due to the presence of cryptic RBD epitopes that are not accessible in the context of the full-length spike protein, or the respective sybodies may recognize the vYFP portion of the RBD-vYFP construct, though the selection procedure clearly disfavors the latter explanation. Importantly, background binding to the dummy protein MBP was not observed for any of the analyzed sybodies, clearly showing that the binders are highly specific. We then sequenced 72 sybodies that were ELISA-positive against RBD-vYFP as well as the full-length spike (12 for each of the 6 selection reactions numbered from Sb#1-72, see also Fig. 1B).

Sequence analysis

Sequencing results of 70 out of 72 sybody clones were unambiguous. Out of these 70 clones, 63 were found to be unique and the respective clone names are indicated in the ELISA figure (Fig. 2, Table 21). Of note, there were no duplicate binders identified in both selection variants, indicating that the two separate selection streams gave rise to completely different arrays of sybodies. As an additional note, one sybody identified from the supposed convex library turned out to belong to the concave library; spill-over of sybodies across libraries is occasionally observed. Hence, there was a total of 23 concave, 22 loop and 18 convex sybodies, which were then aligned according to their library origin (Figs. 3-5). As a final analysis, all sybody sequences were aligned to generate a phylogenetic tree, which shows a

bioRxiv preprint doi: https://doi.org/10.1101/2020.04.16.045419; this version posted April 18, 2020. The copyright holder for this preprint (which was not certified by peer review) is the author/funder, who has granted bioRxiv a license to display the preprint in perpetuity. It is made available under aCC-BY 4.0 International license.

clear segregation across the three libraries and indicates a large sequence variability of the identified sybodies (Fig. 6).

Conclusion and outlook

We have demonstrated the ability of our rapid *in vitro* selection platform to generate sybodies against the SARS-CoV-2 RBD, within a two-week timeframe. We anticipate that the presented panel of anti-RBD sybodies could be of use in the design of urgently required therapeutics to mitigate the COVID-19 pandemic, particularly in the development of inhalable prophylactic formulations [37]. We have attempted to provide a complete account of the generation of these molecules, including full sequences and detailed methods, such that other researchers may contribute to their ongoing analysis. We are currently engaging in additional characterization of these sybodies, including affinity determination, ACE2 competition analysis and pseudovirus neutralization assays, and will provide updates to this manuscript as new data is acquired. Furthermore, while we have tested these anti-RBD sybodies for interaction with full wild-type SARS-CoV-2 spike protein, we will re-screen our selection pools against an engineered spike variant that stably maintains a trimeric pre-fusion conformation [13, 14, 31]. In the longer-term outlook, sybodies resulting from future selection campaigns, targeting additional spike epitopes, will be coupled to the present anti-RBD sybodies to generate polyvalent constructs; such multi-specific designs may be crucial for the evasion of SARS-CoV-2 escape mutants. Finally, our recently described flycode technology will be employed for deeper interrogation of selection pools, in order to facilitate discovery of exceptional sybodies that possess very low off-rates or recognize rare epitopes [41].

METHODS

Cloning, expression and purification of SARS-CoV-2 proteins

A gene encoding SARS-CoV-2 residues Pro330—Gly526 (RBD, GenBank accession QHD43416.1), downstream from a modified N-terminal human serum albumin secretion signal [42], was chemically synthesized (GeneUniversal). This gene was subcloned using FX technology [43] into a custom mammalian expression vector [44], appending a C-terminal 3C protease cleavage site, myc tag, venus YFP[45], and streptavidin-binding peptide [46] onto the open reading frame (RBD-vYFP). 100–250 mL of suspension-adapted Expi293 cells (Thermo) were transiently transfected using Expifectamine according to the manufacturer protocol (Thermo), and expression was continued for 4–5 days in a humidified environment at 37°C, 8% CO_2. Cells were pelleted (500*g*, 10 min), and culture supernatant was filtered (0.2 µm mesh size) before being passed three times over a gravity column containing NHS-agarose beads covalently coupled to the anti-GFP nanobody 3K1K [39], at a resin:culture ratio of 1ml resin per 100ml expression culture. Resin was washed with 20 column-volumes of RBD buffer (phosphate-buffered saline, pH 7.4, supplemented with additional 0.2M NaCl), and RBD-vYFP was eluted with 0.1 M glycine, pH 2.5, via sequential 0.5 ml fractions, without prolonged incubation of resin with the acidic elution buffer. Fractionation tubes were pre-filled with 1/10 vol 1M Tris, pH 9.0 (50 µl), such that elution fractions were immediately pH-neutralized. Fractions containing RBD-vYFP were pooled, concentrated, and stored at 4°C. Purity was estimated to be >95%, based on SDS-PAGE (not shown). Yield of RBD-vYFP was approximately 200–300 µg per 100 ml expression culture. A second purified RBD construct, consisting of SARS-CoV-2 residues Arg519—Phe541 fused to a murine IgG1 Fc

bioRxiv preprint doi: https://doi.org/10.1101/2020.04.16.045419; this version posted April 18, 2020. The copyright holder for this preprint (which was not certified by peer review) is the author/funder, who has granted bioRxiv a license to display the preprint in perpetuity. It is made available under aCC-BY 4.0 International license.

domain (RBD-Fc) expressed in HEK293 cells, was purchased from Sino Biological (Catalogue number: 40592-V05H, 300 µg were ordered). Purified full-length spike ectodomain (ECD) comprising S1 and S2 (residues Val16—Pro1213) with a C-terminal His-tag and expressed in baculovirus-insect cells was purchased from Sino Biological (Catalogue number: 40589-V08B1, 700 µg were ordered).

Biotinylation of target proteins

To remove amines, all proteins were first extensively dialyzed against RBD buffer. Proteins were concentrated to 25 µM using Amicon Ultra concentrator units with a molecular weight cutoff of 30 – 50 kDa. Subsequently, the proteins were chemically biotinylated for 30 min at 25°C using NHS-Biotin (Thermo Fisher, #20217) added at a 10-fold molar excess over target protein. Immediately after, both samples were dialyzed against TBS pH 7.5. During these processes (first dialysis/ concentrating/ biotinylation/ second dialysis), 20 %, 30 % and 65 % of the RBD-vYFP, RBD-Fc and ECD, respectively were lost due to sticking to the concentrator filter or due to aggregation. Biotinylated samples were diluted to 5 µM in TBS pH7.5, 10 % glycerol and stored in small aliquots at -80°C.

Sybody selections

Sybody selections with the three sybody libraries concave, loop and convex were carried out as described in detail before [36]. In short, one round of ribosome display followed by two rounds of phage display were carried out. Binders were selected against two different constructs of the SARS-CoV-2 RBD; an RBD-vYFP fusion and an RBD-Fc fusion. MBP was used as background control to determine the enrichment score by qPCR [36]. In order to avoid enrichment of binders against the fusion proteins (YFP and Fc), we switched the two targets after ribosome display (Fig. 1B). For the off-rate selections we did not use non-biotinylated target proteins as described in the standard protocol, because we did not have enough purified protein at hand to do so. Instead we sub-cloned all three libraries for both selections after the first round of phage display into the pSb_init vector (10^8 clones) and expressed the six pools in *E. coli* MC1061 cells. Then the pools corresponding to the same selection were pooled for purification. The two final pools were purified by Ni-NTA resin using gravity flow columns, followed by buffer exchange of the main peak fraction using a desalting PD10 column in TBS pH 7.5 to remove imidazole. The pools were eluted with 3.2 ml instead of 3.5 ml TBS pH 7.5 in order to ensure complete buffer exchange. These two purified pools were used for the off-rate selection in the second round of phage display at concentrations of approximately 390 µM for selection variant 1 (RBP-Fc) and 450 µM for selection variant 2 (RBP-YFP). The volume used for off-rate selection was 500 µl. Just before the pools were used for the off-rate selection, 0.5% BSA and 0.05% Tween-20 was added to each sample. Off-rate selections were performed for 3 minutes.

Sybody identification by ELISA

ELISAs were performed as described in detail before [36]. 47 single clones were analyzed for each library of each selection. Since the RBD-Fc construct was incompatible with our ELISA format due to the inclusion of Protein A to capture an α-myc antibody, ELISA was performed only for the RBD-vYFP (50 nM) and the ECD (25 nM). As negative control to assess background binding of sybodies, we used biotinylated MBP (50 nM). 72 positive ELISA hits were sequenced (Microsynth, Switzerland).

bioRxiv preprint doi: https://doi.org/10.1101/2020.04.16.045419; this version posted April 18, 2020. The copyright holder for this preprint (which was not certified by peer review) is the author/funder, who has granted bioRxiv a license to display the preprint in perpetuity. It is made available under aCC-BY 4.0 International license.

TABLES

Table 1 – Key parameters of selection process

Selection variant/library	Enrichment Phage display#1	Enrichment Phage display#2	Number of ELISA hits against RBD/ECD (out of total analyzed)	Number of unique binders (out of total sequenced)
Variant 1 vYFP-Fc-Fc				
Concave (Sb#1-12)	1.8	204.9	46/45 (47)	12 (12)
Loop (Sb#25-36)	1.5	52.5	46/33 (47)	12 (12)
Convex (Sb#49-60) [1)]	1.3	10.1	38/31 (47)	9 (12)
Variant 2 Fc-vYFP-vYFP				
Concave (Sb#13-24)	7.0	263.1	47/37 (47)	10 (12) [2)]
Loop (Sb#37-48)	3.0	44.9	44/36 (47)	10 (12)
Convex (Sb#61-72)	1.2	47.7	46/41 (47)	10 (12)

[1)] Sb#51 belongs to the concave library (spill-over). [2)] Two sequencing reactions failed.

Table 2 – Sybody protein sequences

Sb#1	QVQLVESGGGLVQAGGSLRLSCAASGFPVRKANMHWYRQAPGKEREWVAAIMSKGEQTVYADSVE GRFTISRDNAKNTVYLQMNSLKPEDTAVYYCRVFVGWHYFGQGTQVTVS
Sb#2	QVQLVESGGGLVQAGGSLRLSCATSGFPVYQANMHWYRQAPGKEREWVAAIQSYGDGTHYADSVK GRFTISRDNAKNTVYLQMNSLKPEDTAVYYCRAVYVGMHYFGQGTQVTVS
Sb#3	QVQLVESGGGLVQAGGSLRLSCAASGFPVNYKTMWWYRQAPGKEREWVAAIWSYGHTTHYADSVK GRFTISRDNAKNTVYLQMNSLKPEDTAVYYCVVWVGHNYEGQGTQVTVS
Sb#4	QVQLVESGGGLVQAGGSLRLSCAASGFPVYAQNMHWYRQAPGKEREWVAAIYSHGYWTLYADSVK GRFTISRDNAKNTVYLQMNSLKPEDTAVYYCEVQVGAWYTGQGTQVTVS
Sb#5	QVQLVESGGGLVQAGGSLRLSCAASGFPVFSGHMHWYRQAPGKEREWVAAILSNGDSTHYADSVK GRFTISRDNAKNTVYLQMNSLKPEDTAVYYCRVHVGAHYFGQGTQVTVS
Sb#6	QVQLVESGGGLVQAGGSLRLSCAASGFPVEQGRMYWYRQAPGKEREWVAAIISHGTVTVYADSVK GRFTISRDNAKNTVYLQMNSLKPEDTAVYYCYVYVGAQYWGQGTQVTVS
Sb#7	QVQLVESGGGLVQAGGSLRLSCAASGFPVLFTYMHWYRQAPGKEREWVAAIWSSGNSTWYADSVK GRFTISRDNAKNTVYLQMNSLKPEDTAVYYCFVKVGNWYAGQGTQVTVS
Sb#8	QVQLVESGGGLVQAGGSLRLSCAASGFPVNAGNMHWYRQAPGKEREWVAAIQSYGRTTYYADSVK GRFTISRDNAKNTVYLQMNSLKPEDTAVYYCRVFVGMHYFGQGTQVTVS
Sb#9	QVQLVESGGGLVQAGGSLRLSCAASGFPVSSSTMTWYRQAPGKEREWVAAINSYGWETHYADSVK GRFTISRDNAKNTVYLQMNSLKPEDTAVYYCYVYVGGSYIGQGTQVTVS
Sb#10	QVQLVESGGGLVQAGGSLRLSCAASGFPVQSHYMRWYRQAPGKEREWVAAIESTGHHTAYADSVK GRFTISRDNAKNTVYLQMNSLKPEDTAVYYCTVYVGYEYHGQGTQVTVS
Sb#11	QVQLVESGGGLVQAGGSLRLSCAASGFPVETENMHWYRQAPGKEREWVAAIYSHGMWTAYADSVK GRFTISRDNTKNTVYLQMNSLKPEDTAVYYCEVEVGKWYFGQGTQVTVS
Sb#12	QVQLVESGGGLVQAGGSLRLSCAASGFPVKASRMYWYRQAPGKEREWVAAIQSFGEVTWYADSVK GRFTISRDNAKNTVYLQMNSLKPEDTAVYYCYVWVGQEYWGQGTQVTVS
Sb#13	QVQLVESGGGLVQAGGSLRLSCAASGFPVYASNMHWYRQAPGKEREWVAAIESQGYMTAYADSVK GRFTISRDNAKNTVYLQMNSLKPEDTAVYYCWVIVGEYYVGQGTQVTVS

bioRxiv preprint doi: https://doi.org/10.1101/2020.04.16.045419; this version posted April 18, 2020. The copyright holder for this preprint (which was not certified by peer review) is the author/funder, who has granted bioRxiv a license to display the preprint in perpetuity. It is made available under aCC-BY 4.0 International license.

Sb#14	QVQLVESGGGLVQAGGSLRLSCAASGFPVQAREMEWYRQAPGKEREWVAAIKSTGTYTAYAYSVK GRFTISRDNAKNTVYLQMNSLKPEDTAVYYCYVYVGSSYIGQGTQVTVS
Sb#15	QVQLVESGGGLVQAGGSLRLSCAASGFPVKNFEMEWYRKAPGKEREWVAAIQSGGVETYYADSVK GRFTISRDNAKNTVYLQMNSLKPEDTAVYYCFVYVGRSYIGQGTQVTVS
Sb#16	QVQLVESGGGLVQAGGSLRLSCAASGFPVAYKTMWWYRQAPGKEREWVAAIESYGIKWTRYADSV KGRFTISRDNAKNTVYLQMNSLKPEDTAVYYCIVWVGAQYHGQGTQVTVS
Sb#17	QVQLVESGGGLVQAGGSLRLSCAASGFPVAGRNMWWYRQAPGKEREWVAAIYSSGTYTEYADSVK GRFTISRDNAKNTVYLQMNSLKPEDTAVYYCHVWVGSLYKGQGTQVTVS
Sb#18	QVQLVESGGGLVQAGGSLRLSCAASGFPVKHARMWWYRQAPGKEREWVAAIDSHGDTTWYADSVK GRFTISRDNAKNTVYLQMNSLKPEDTAVYYCYVYVGASYWGQGTQVTVS
Sb#19	QVQLVESGGGLVQAGGSLRLSCAASGFPVNSHEMTWYRQAPGKEREWVAAIQSTGTVTEYADSVK GRFTISRDNAKNTVYLQMNSLKPEDTAVYYCYVYVGSSYLGQGTQVTVS
Sb#20	QVQLVESGGGLVQAGGSLRLSCAASGFPVEQREMEWYRQAPGKEREWVAAIDSNGNYTFYADSVK GRFTISRDNAKNTVYLQMNSLKPEDTAVYYCYVYVGKSYIGQGTQVTVS
Sb#21	QVQLVESGGGLVQAGGSLRLSCAASGFPVKHHWMFWYRQAPGKEREWVAAIKSYGYGTEYADSVK GRFTISRDNAKNTVYLQMNSLKPEDTAVYYCFVGVGTHYAGQGTQVTVS
Sb#23	QVQLVESGGGLVQAGGSLRLSCAASGFPVYAAEMEWYRQAPGKEREWVAAISSQGTITYYADSVK GRFTISRDNAKNTVYLQMNSLKPEDTAVYYCFVYVGKSYIGQGTQVSVS
Sb#25	QVQLVESGGGLVQAGGSLRLSCAASGFPVHAWEMAWYRQAPGKEREWVAAIRSFGSSTHYADSVK GRFTISRDNAKNTVYLQMNSLKPEDTAVYYCNVKDFGTHHYAYDYWGQGTQVTVS
Sb#26	QVQLVESGGGLVQAGGSLRLSCAASGFPVNTWWMHWYRQAPGKEREWVAAITSWGFRTYYADSVK GRFTISRDNAKNTVYLQMNSLKPEDTAVYYCNVKDKGMAVQWYDYWGQGTQVTVS
Sb#27	QVQLVESGGGLVQAGGSLRLSCAASGFPVYNTWMEWYRQAPGKEREWVAAITSHGYKTYYADSVK GRFTISRDNAKNTVYLQMNSLKPEDTAVYYCNVKDEGDMFTAYDYWGQGTQVTVS
Sb#28	QVQLVESGGGLVQAGGSLRLSCAASGFPVYHSTMFWYRQAPGKEREWVAAIYSSGQHTYYADSVK GRFTISRDNAKNTVYLQMNSLKPEDTAVYYCNVKDSGQWRQEYDYWGQGTQVTVS
Sb#29	QVQLVESGGGLVQAGGSLRLSCAASGFPVEHEMAWYRQAPGKEREWVAAIRSMGRKTLYADSVKG RFTISRDNAKNTVYLQMNSLKPEDTAVYYCNVKDFGYTWHEYDYWGQGTQVTVS
Sb#30	QVQLVESGGGLVQAGGSLRLSCAASGFPVTMAWMWWYRQAPGKEREWVAAIRSEGVRTYYADSVK GRFTISRDNAKNTVYLQMNSLKPEDTAVYYCNVKDYGQAHAYYDYWGQGTQVTVS
Sb#31	QVQLVESGGGLVQAGGSLRLSCAASGFPVNSHFMEWYRQAPGKEREWVAAIQHSSGFHTYYADSV KGRFTISRDNAKNTVYLQMNSLKPEDTAVYYCNVKDTGTTEDYDYWGQGTQVTVS
Sb#32	QVQLDESGGGLVQAGGSLRLSCAASGFPVYHAWMEWYRQAPGKEREWVAAITSSGRHTYYADSVK GRFTISRDNAKNTVYLQMNSLKPEDTAVYYCNVKDAGRVYNSYDYWGQGTQVTVS
Sb#33	QVQLVESGGGLVQAGGSLRLSCAASGFPVAHAWMEWYRQAPGKEREWVAAITSYGYKTYYADSVK GRFTISRDNAKNTVYLQMNSLKPEDTAVYYCNVKDTGTYRFYYDYWGQGTQVTVS
Sb#34	QVQLVESGGGLVQAGGSLRLSCAASGFPVWNQTMVWYRQAPGKEREWVAAIWSMGHTYYADSVKG RFTISRDNAKNTVYLQMNSLKPEDTAVYYCNVKDAGVYNRYYDYWGQGTQVTVS
Sb#35	QVQLVESGGGLVQAGGSLRLSCAASGFPVEHYWMEWYRQAPGKEREWVAAITSFGYRTYYADSVK GRFTISRDNAKNTVYLQMNSLKPEDTAVYYCNVKDWGFASHAYDYWGQGIQVTVS
Sb#36	QVQLVESGGGLVQAGGSLRLSCAASGFPEIAWEMAWYRQAPGKEREWVAAIRSFGERTLYADSVK GRFTISRDNAKNTVYLQMNSLKPEDTAVYYCNVKDFGWQHQEYDYWGQGTQVTVS
Sb#37	QVQLVESGGGLVQAGGSLRLSCAASGFPVYHAYMEWYRQAPGKEREWVAAIYSNGEHTYYADSVK GRFTISRDNAKNTVYLQMNSLKPEDTAVYYCNVKDSGSFNQAYDYWGQGTQVTVS
Sb#38	QVQLVESGGGLVQAGGSLRLSCAASGFPVEWSHMHWYRQAPGKEREWVAAIVSKGGYTLYADSVK GRFTISRDNAKNTVYLQMNSLKPEDTAVYYCNVKDYGVHFKRYDYWGQGTQVTVI
Sb#39	QVQLVESGGGLVQAGGSLRLSCAASGFPVFHVWMEWYRQAPGKEREWVAAIDSAGWHTYYADSVK GRFTISRDNAKNTVYLQMNSLKPEDTAVYYCNVKDAGNTTSAYDYWGQGTQVTVS
Sb#40	QVQLVESGGGLVQAGGSLRLSCAASGFPVYYNWMEWYRQAPGKEREWVAAIHSNGDETFYADSVK GRFTISRDNAKNTVYLQMNSLKPEDTAVYYCNVKDIDAEAYAYDYWGQGTQVTVS
Sb#41	QVQLVESGGGLVQAGGSLRLSCAASGFPVYHVWMEWYRQAPGKEREWVAAITSSGSHTYYADSVK GRFTISRDNAKNTVYLQMNSLKPEDTAVYYCNVKDSGQWRVQYDYWGQGTQVTVS

bioRxiv preprint doi: https://doi.org/10.1101/2020.04.16.045419; this version posted April 18, 2020. The copyright holder for this preprint (which was not certified by peer review) is the author/funder, who has granted bioRxiv a license to display the preprint in perpetuity. It is made available under aCC-BY 4.0 International license.

Sb#42	QVQLVESGGGLVQAGGSLRLSCAASGFPVYWHHMHWYRQAPGKEREWVAAIISWGWYTTYADSVK GRFTISRDNAKNTVYLQMNSLKPEDTAVYYCNVKDHGAQNQMYDYWGQGTQVTVS
Sb#45	QVQLVESGGGLVQAGGSLRLSCAASGFPVYRDRMAWYRQAPGKEREWVAAIYSAGQQTRYADSVK GRFTISRDNAKNTVYLQMNSLKPEDTAVYYCNVKDVGHHYEYYDYWGQGTQVTVS
Sb#46	QVQLVESGGGLVQAGGSLRLSCAASGFPVDNGYMHWYRQAPGKEREWVAAIDSYGWHTIYADSVK GRFTISRDNAKNTVYLQMNSLKPEDTAVYYCNVKDKGQMRAAYDYWGQGTQVTVS
Sb#47	QVQLVESGGGLVQAGGSLRLSCAASGFPVSWHSMYWYRQAPGKEREWVAAIFSEGDWTYYADSVK GRFTISRDNAKNTVYLQMNSLKPEDTAVYYCNVKDYGSSYYKYDYWGQGTQVTVS
Sb#48	QVQLVESGGGLVQAGGSLRLSCAASGFPVSQSVMAWYRQAPGKEREWVAAIYSKGQYTHYADSVK GRFTISRDNAKNTVYLQMNSLKPEDTAVYYCNVKDAGSSYWDYDYWGQGTQVTVS
Sb#49	QVQLVESGGGSVQAGGSLRLSCAASGSIGQIEYLGWFRQAPGKEREGVAALNTWTGRTYYADSVK GRFTVSLDNAKNTVYLQMNSLKPEDTALYYCAAARWGRTKPLNTYYYSYWGQGTPVTVS
Sb#50	QVQLVESGGGSVQAGGSLRLSCAASGYIDKIVYLGWFRQAPGKEREGVAALYTLSGHTYYADSVK GRFTVSLDNAKNTVYLQMNSLKPEDTALYYCAAATEGHAHALYRLHYYWGQGTQVTVS
Sb#51	QVQLVESGGGLVQAGGSLRLSCAASGFPVYQGEMHWYRQAPGKEREWVAAIRSTGVQTWYADSVK GRFTISRDNAKNTVYLQMNSLKPEDTAVYYCRVWVGTHYFGQGTQVTVS
Sb#52	QVQLVESGGGSVQAGGSLRLSCAASGNIQRIYYLGWFRQAPGKEREGVAALMTYTGHTYYADSVK GRFTVSLDNAKNTVYLQMNSLKPEDTALYYCAAAYVGAENPLPYSMYGYWGQGTQVTVS
Sb#53	QVQLVESGGGSVQAGGSLRLSCAASGQISHIKYLGWFRQAPGKEREGVAALITRWGQTYYADSVK GRFTVSLDNAKNTVYLQMNSLKPEDTALYYCAAADYGASDPLWFIHYLYWGQGTQVTVS
Sb#55	QVQLVESGGGSVQAGGSLRLSCAASGKIWTIKYLGWFRQAPGKEREGVAALMTRWGYTYYADSVK GRFTVSLDNAKNTVYLQMNSLKPEDTALYYCAAANYGSNFPLAEEDYWYWGQGTQVTVS
Sb#56	QVQLVESGGGSVQAGGSLRLSCAASGNISQIHYLGWFRQAPGKEREGVAALNTDYGYTYYADSVK GRFTVSLDNAKNTVYLQMNSLKPEDTALYYCAAAYYFGDDIPLWWEAYSYWGQGTQVTVS
Sb#58	QVQLVESGGGSVQAGGSLRLSCAASGNISTIEYLGWFRQAPGKEREGVAALYTWHGQTYYADSVK GRFTVSLDNAKNTVYLQMNSLKPEDTALYYCAAARWGRHMPLSATEYSYWGQGTQVTVS
Sb#59	QVQLVESGGGSVQAGGSLRLSCAASGNIESIYYLGWFRQAPGKEREGVAALWTGDGETYYADSVK GRFTVSLDNAKNTVYLQMNSLKPEDTALYYCAAAAWGNSAPLTTYRYYYWGQGTQVTVS
Sb#61	QVQLVESGGGSVQAGGSLRLSCAASGFIYGITYLGWFRQAPGKEREGVAALVTWNGQTYYADSVK GRFTVSLDNAKNTVYLQMNSLKPEDTALYYCAAADWGYDWPLWDEWYWYWGQGTQVTVS
Sb#62	QVQLVESGGGSVQAGGSLRLSCAASGTIADIKYLGWFRQAPGKEREGVAALMTRWGSTYYADSVK GRFTVSLDNAKNTVYLQMNSLKPEDTALYYCAAANYGANYPLYSQQYSYWGQGTQVTVS
Sb#63	QVQLVESGGGSVQAGGSLRLSCAASGSISSIKYLGWFRQAPGKEREGVAALMTRWGMTYYADSVK GRFTVSLDNAKNTVYLQMNSLKPEDTALYYCAAANYGANEPLQYTHYNYWGQGTQVTVS
Sb#64	QVQLVESGGGSVQAGGSLRLSCAASGEIESIFYLGWFRQAPGKEREGVAALYTYVGQTYYADSVK GRFTVSLDNAKNTVYLQMNSLKPEDTALYYCAAASYGAAHPLSIMRYYYWGQGTQVTVS
Sb#65	QVQLVESGGGSVQAGGSLRLSCAASGTIAHIKYLGWFRQAPGKEREGVAALMTKWGQTYYADSVK GRFTVSLDNAKNTVYLQMNSLKPEDTALYYCAAASYGANFPLKASDYSYWGQGTQVTVS
Sb#66	QVQLVESGGGSVQAGGSLRLSCAASGSIQAITYLGWFRQAPGKEREGVAALVTWNGQTYYADSVK GRFTVSLDNAKNTVYLQMNSLKPEDTALYYCAAADWGYDWPLWDEWYWYWGQGTQVTVS
Sb#67	QVQLVESGGGSVQAGGSLRLSCAASGSISSITYLGWFRQAPGKEREGVAALVTYSGNTYYADSVK GRFTVSLDNAKNTVYLQMNSLKPEDTALYYCAAATWGHSWPLYNDEYWYWGQGSQVTVS
Sb#68	QVQLVESGGGSVQAGGSLRLSCAASGSISSITYLGWFRQAPGKEREGVAALITVNGHTYYADSVK GRFTVSLDNAKNTVYLQMNSLKPEDTALYYCAAAAWGYAWPLHQDDYWYWGQGTQVTVS
Sb#69	QVQLVESGGGSVQAGGSLRLSCAASGSISSITYLGWFRQAPGKEREGVAALNTFNGTTYYADSVK GRFTVSLDNAKNTVYLQMNSLKPEDTALYYCAAATWGYSWPLIAEYNWYWGQGTQVTVS
Sb#71	QVQLVESGGGSVQAGGSLRLSCAASGSISSITYLGWFRQAPGKEREGVAALKTQAGFTYYADSVK GRFTVSLDNAKNTVYLQMNSLKPEDTALYYCAAANWGYSWPLYEADDWYWGQGTQVTVS

bioRxiv preprint doi: https://doi.org/10.1101/2020.04.16.045419; this version posted April 18, 2020. The copyright holder for this preprint (which was not certified by peer review) is the author/funder, who has granted bioRxiv a license to display the preprint in perpetuity. It is made available under aCC-BY 4.0 International license.

DATA AVAILABILITY STATEMENT

We are currently unable to ship plasmids and purified proteins. We will further analyze the identified sybodies and will make the highest affinity binders available through Addgene (will take 3-4 weeks until available). Please feel free to synthesize sybody genes based on the protein sequences provided here.

REFERENCES

1. Kwok, K.O., et al., *Herd immunity - estimating the level required to halt the COVID-19 epidemics in affected countries.* J Infect, 2020.
2. Liu, Y., et al., *The reproductive number of COVID-19 is higher compared to SARS coronavirus.* J Travel Med, 2020. **27**(2).
3. Zhang, S., et al., *Estimation of the reproductive number of novel coronavirus (COVID-19) and the probable outbreak size on the Diamond Princess cruise ship: A data-driven analysis.* Int J Infect Dis, 2020. **93**: p. 201-204.
4. Bai, Y., et al., *Presumed Asymptomatic Carrier Transmission of COVID-19.* JAMA, 2020.
5. Wu, J.T., et al., *Estimating clinical severity of COVID-19 from the transmission dynamics in Wuhan, China.* Nature Medicine, 2020: p. 1-5.
6. Wickramasinghe, N.C., et al., *Predicting the Future Trajectory of COVID-19.* Virology, 2020. **4**(1).
7. Ahmed, S.F., A.A. Quadeer, and M.R. McKay, *Preliminary Identification of Potential Vaccine Targets for the COVID-19 Coronavirus (SARS-CoV-2) Based on SARS-CoV Immunological Studies.* Viruses, 2020. **12**(3).
8. Chen, W.-H., et al., *The SARS-CoV-2 vaccine pipeline: An overview.* Current Tropical Medicine Reports, 2020: p. 1-4.
9. Mitja, O. and B. Clotet, *Use of antiviral drugs to reduce COVID-19 transmission.* Lancet Glob Health, 2020.
10. Wang, C., et al., *A novel coronavirus outbreak of global health concern.* Lancet, 2020. **395**(10223): p. 470-473.
11. Menachery, V.D., et al., *A SARS-like cluster of circulating bat coronaviruses shows potential for human emergence.* Nat Med, 2015. **21**(12): p. 1508-13.
12. Li, F., *Structure, Function, and Evolution of Coronavirus Spike Proteins.* Annu Rev Virol, 2016. **3**(1): p. 237-261.
13. Wrapp, D., et al., *Cryo-EM structure of the 2019-nCoV spike in the prefusion conformation.* Science, 2020. **367**(6483): p. 1260-1263.
14. Walls, A.C., et al., *Structure, function, and antigenicity of the SARS-CoV-2 spike glycoprotein.* Cell, 2020.
15. Hoffmann, M., et al., *SARS-CoV-2 Cell Entry Depends on ACE2 and TMPRSS2 and Is Blocked by a Clinically Proven Protease Inhibitor.* Cell, 2020.
16. Hulswit, R.J.G., et al., *Human coronaviruses OC43 and HKU1 bind to 9-O-acetylated sialic acids via a conserved receptor-binding site in spike protein domain A.* Proc Natl Acad Sci U S A, 2019. **116**(7): p. 2681-2690.
17. Kirchdoerfer, R.N., et al., *Pre-fusion structure of a human coronavirus spike protein.* Nature, 2016. **531**(7592): p. 118-21.

bioRxiv preprint doi: https://doi.org/10.1101/2020.04.16.045419; this version posted April 18, 2020. The copyright holder for this preprint (which was not certified by peer review) is the author/funder, who has granted bioRxiv a license to display the preprint in perpetuity. It is made available under aCC-BY 4.0 International license.

18. Yuan, Y., et al., *Cryo-EM structures of MERS-CoV and SARS-CoV spike glycoproteins reveal the dynamic receptor binding domains.* Nat Commun, 2017. **8**: p. 15092.
19. Harrison, S.C., *Viral membrane fusion.* Virology, 2015. **479-480**: p. 498-507.
20. Walls, A.C., et al., *Unexpected Receptor Functional Mimicry Elucidates Activation of Coronavirus Fusion.* Cell, 2019. **176**(5): p. 1026-1039 e15.
21. He, Y., et al., *Identification of immunodominant sites on the spike protein of severe acute respiratory syndrome (SARS) coronavirus: implication for developing SARS diagnostics and vaccines.* J Immunol, 2004. **173**(6): p. 4050-7.
22. Du, L., et al., *The spike protein of SARS-CoV--a target for vaccine and therapeutic development.* Nat Rev Microbiol, 2009. **7**(3): p. 226-36.
23. Berry, J.D., et al., *Development and characterisation of neutralising monoclonal antibody to the SARS-coronavirus.* J Virol Methods, 2004. **120**(1): p. 87-96.
24. ter Meulen, J., et al., *Human monoclonal antibody combination against SARS coronavirus: synergy and coverage of escape mutants.* PLoS Med, 2006. **3**(7): p. e237.
25. Jiang, L., et al., *Potent neutralization of MERS-CoV by human neutralizing monoclonal antibodies to the viral spike glycoprotein.* Sci Transl Med, 2014. **6**(234): p. 234ra59.
26. He, Y., et al., *Cross-neutralization of human and palm civet severe acute respiratory syndrome coronaviruses by antibodies targeting the receptor-binding domain of spike protein.* J Immunol, 2006. **176**(10): p. 6085-92.
27. He, Y., et al., *Receptor-binding domain of severe acute respiratory syndrome coronavirus spike protein contains multiple conformation-dependent epitopes that induce highly potent neutralizing antibodies.* J Immunol, 2005. **174**(8): p. 4908-15.
28. Zhao, G., et al., *A Novel Nanobody Targeting Middle East Respiratory Syndrome Coronavirus (MERS-CoV) Receptor-Binding Domain Has Potent Cross-Neutralizing Activity and Protective Efficacy against MERS-CoV.* J Virol, 2018. **92**(18).
29. Prabakaran, P., et al., *Structure of severe acute respiratory syndrome coronavirus receptor-binding domain complexed with neutralizing antibody.* J Biol Chem, 2006. **281**(23): p. 15829-36.
30. Wu, Y., et al., *Fully human single-domain antibodies against SARS-CoV-2.* bioRxiv, 2020.
31. Pallesen, J., et al., *Immunogenicity and structures of a rationally designed prefusion MERS-CoV spike antigen.* Proc Natl Acad Sci U S A, 2017. **114**(35): p. E7348-E7357.
32. Muyldermans, S., *Nanobodies: natural single-domain antibodies.* Annu Rev Biochem, 2013. **82**: p. 775-97.
33. Pardon, E., et al., *A general protocol for the generation of Nanobodies for structural biology.* Nat Protoc, 2014. **9**(3): p. 674-93.
34. Rasmussen, S.G., et al., *Structure of a nanobody-stabilized active state of the beta(2) adrenoceptor.* Nature, 2011. **469**(7329): p. 175-80.
35. Zimmermann, I., et al., *Synthetic single domain antibodies for the conformational trapping of membrane proteins.* Elife, 2018. **7**.
36. Zimmermann, I., et al., *Generation of synthetic nanobodies against delicate proteins.* Nat Protoc, 2020.
37. Van Heeke, G., et al., *Nanobodies® as inhaled biotherapeutics for lung diseases.* Pharmacology & therapeutics, 2017. **169**: p. 47-56.
38. Li, F., et al., *Structure of SARS coronavirus spike receptor-binding domain complexed with receptor.* Science, 2005. **309**(5742): p. 1864-8.

bioRxiv preprint doi: https://doi.org/10.1101/2020.04.16.045419; this version posted April 18, 2020. The copyright holder for this preprint (which was not certified by peer review) is the author/funder, who has granted bioRxiv a license to display the preprint in perpetuity. It is made available under aCC-BY 4.0 International license.

39. Kirchhofer, A., et al., *Modulation of protein properties in living cells using nanobodies.* Nat Struct Mol Biol, 2010. **17**(1): p. 133-8.
40. Kuhn, B.T., et al., *Biotinylation of Membrane Proteins for Binder Selections.* Methods Mol Biol, 2020. **2127**: p. 151-165.
41. Egloff, P., et al., *Engineered peptide barcodes for in-depth analyses of binding protein libraries.* Nat Methods, 2019. **16**(5): p. 421-428.
42. Attallah, C., et al., *A highly efficient modified human serum albumin signal peptide to secrete proteins in cells derived from different mammalian species.* Protein Expr Purif, 2017. **132**: p. 27-33.
43. Geertsma, E.R. and R. Dutzler, *A versatile and efficient high-throughput cloning tool for structural biology.* Biochemistry, 2011. **50**(15): p. 3272-8.
44. Brunner, J.D., et al., *X-ray structure of a calcium-activated TMEM16 lipid scramblase.* Nature, 2014. **516**(7530): p. 207-12.
45. Nagai, T., et al., *A variant of yellow fluorescent protein with fast and efficient maturation for cell-biological applications.* Nature biotechnology, 2002. **20**(1): p. 87-90.
46. Keefe, A.D., et al., *One-step purification of recombinant proteins using a nanomolar-affinity streptavidin-binding peptide, the SBP-Tag.* Protein expression and purification, 2001. **23**(3): p. 440-446.

bioRxiv preprint doi: https://doi.org/10.1101/2020.04.16.045419; this version posted April 18, 2020. The copyright holder for this preprint (which was not certified by peer review) is the author/funder, who has granted bioRxiv a license to display the preprint in perpetuity. It is made available under aCC-BY 4.0 International license.

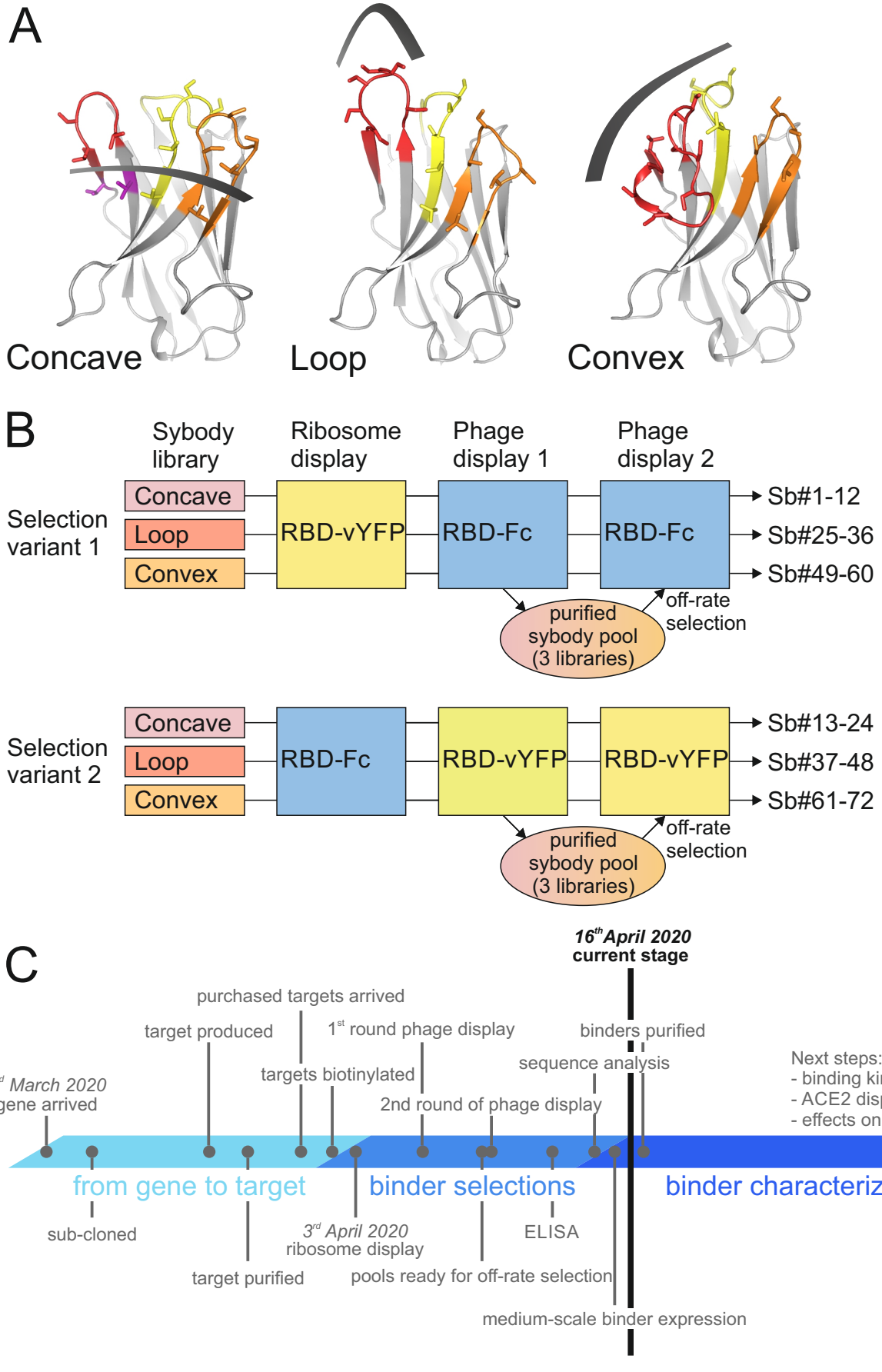

Figure 1

Sybody selections against SARS-CoV-2 RBDs. (**A**) Randomized surface of the three sybody libraries concave, loop and convex. CDR1 in yellow, CDR2 in orange, CDR3 in red. Randomized residues are depicted as sticks. (**B**) Selection scheme. A total of six independent selection reactions were carried out, including a target swap between ribosome display and phage display round. Enriched sybodies of phage display round 1 of all three libraries were expressed and purified as a pool and used to perform an off-rate selection in phage display round 2. (**C**) Time line of this sybody selection process. Please note that this is an intermediate report.

bioRxiv preprint doi: https://doi.org/10.1101/2020.04.16.045419; this version posted April 18, 2020. The copyright holder for this preprint (which was not certified by peer review) is the author/funder, who has granted bioRxiv a license to display the preprint in perpetuity. It is made available under aCC-BY 4.0 International license.

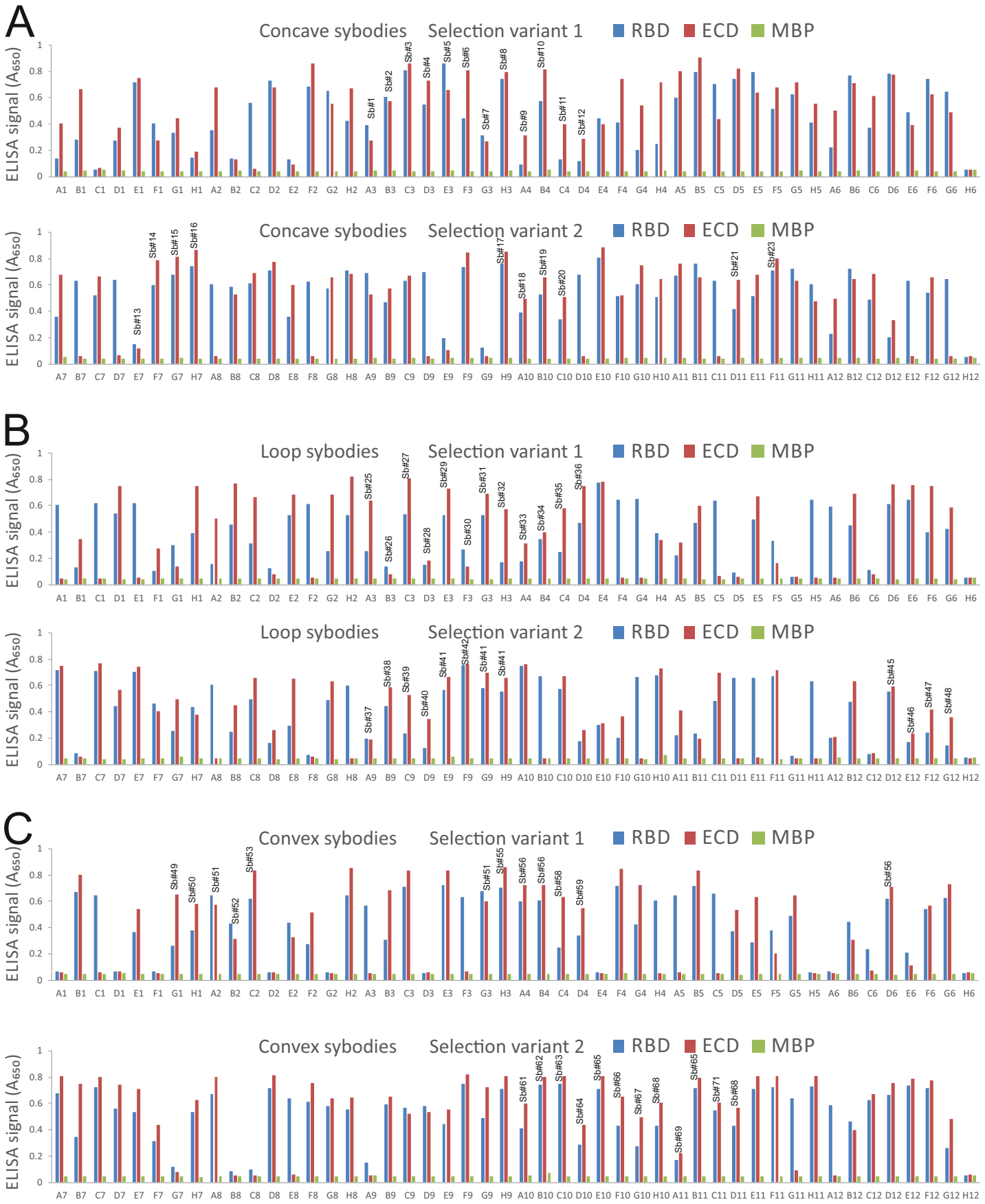

Figure 2

Sybody identification by ELISA. (**A**) Concave sybodies. (**B**) Loop sybodies. (**C**) Convex sybodies. For each of the six independent selection reactions, 47 clones were picked at random and analyzed by ELISA. A non-randomized sybody was used as negative control (wells H6 and H12, respectively). Sybodies that were sequenced are marked with the respective sybody name (Sb_#1-72). Please note that identical sybodies that were found 2-3 times are marked with the same sybody name (e.g. Sb_#41).

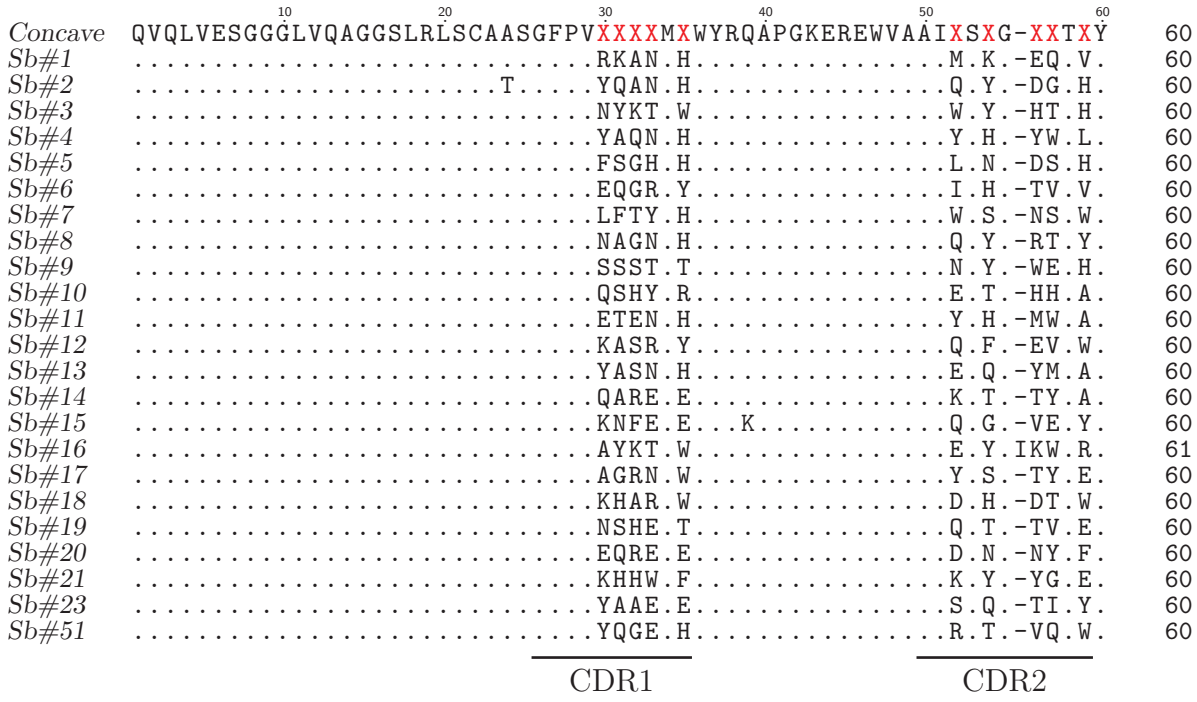

Figure 3

Sequence alignment of concave RBD sybodies.

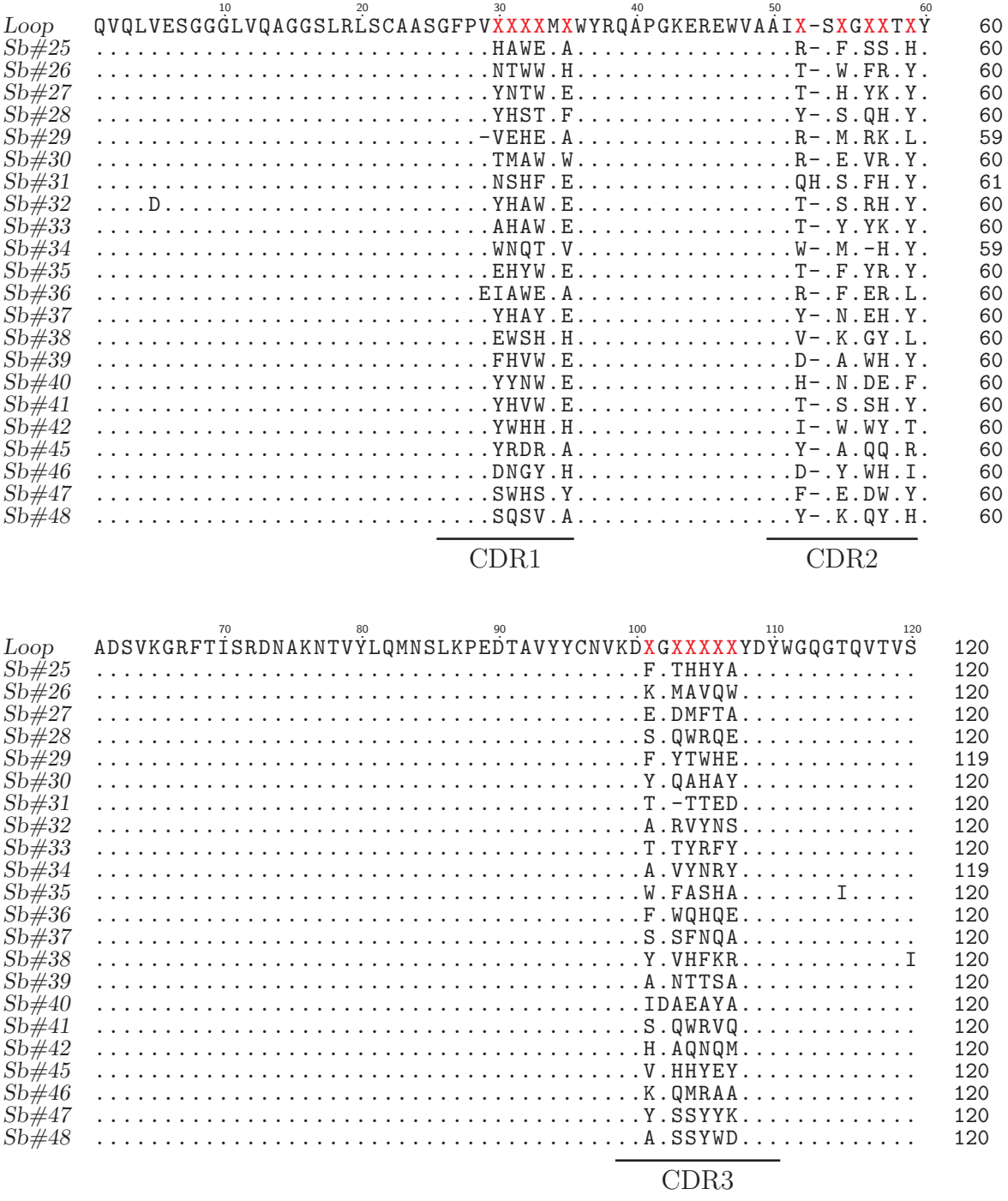

Figure 4

Sequence alignment of loop RBD sybodies.

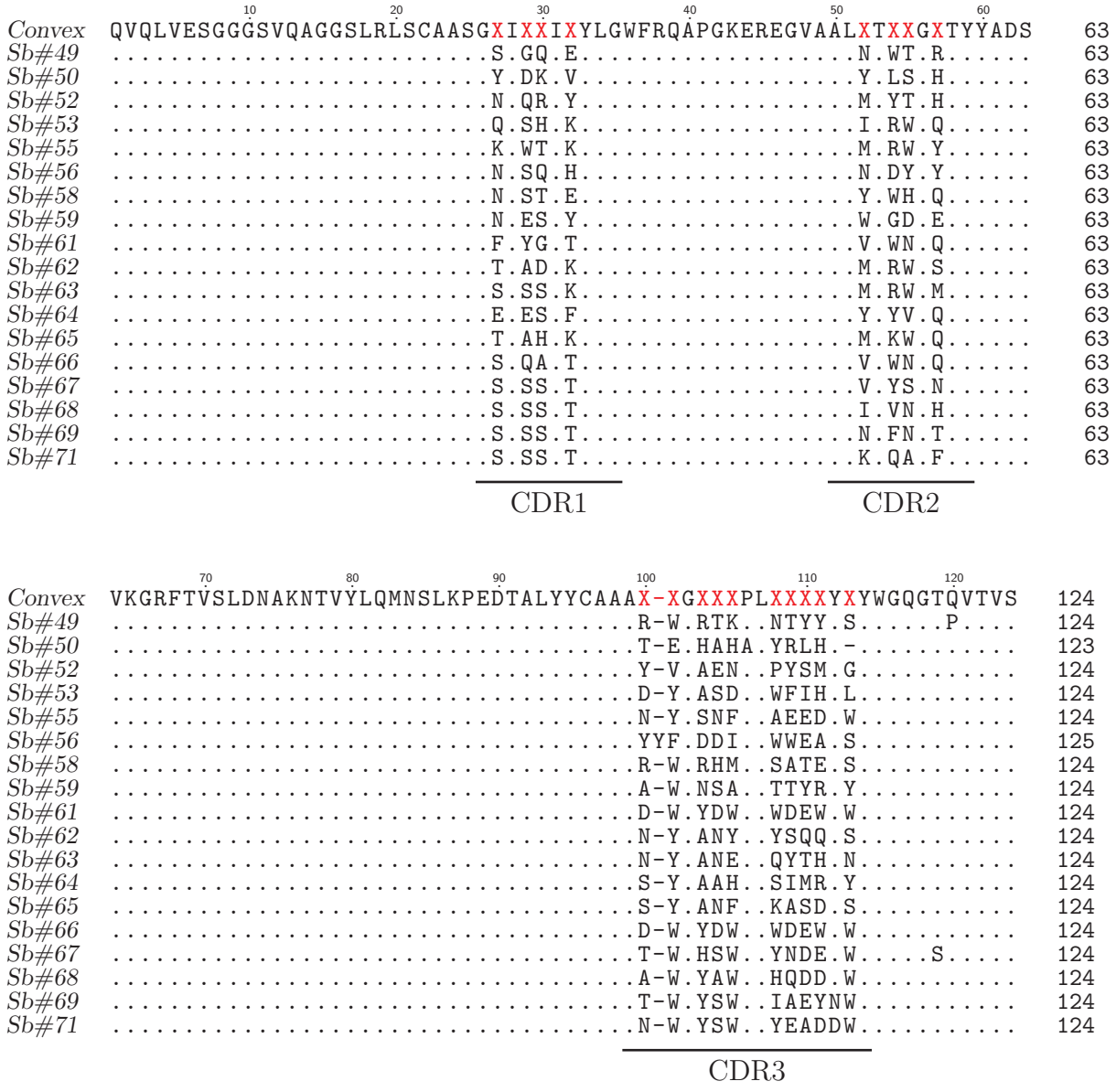

Figure 5

Sequence alignment of convex RBD sybodies.

.

bioRxiv preprint doi: https://doi.org/10.1101/2020.04.16.045419; this version posted April 18, 2020. The copyright holder for this preprint (which was not certified by peer review) is the author/funder, who has granted bioRxiv a license to display the preprint in perpetuity. It is made available under aCC-BY 4.0 International license.

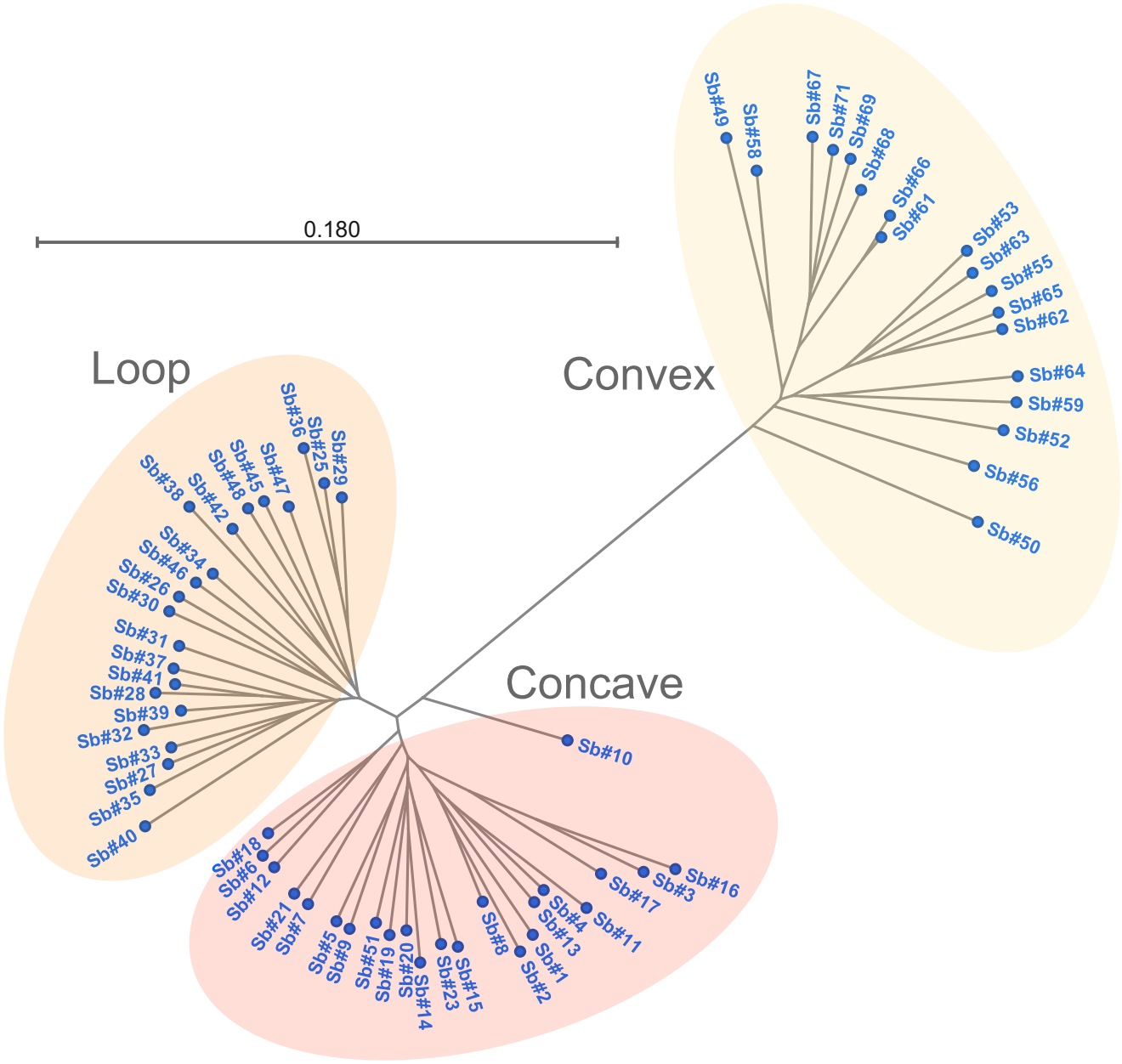

Figure 6

Phylogenetic tree of RBD sybodies. A radial tree was generated in CLC 8.1.3.